Advances in Engineering Research, volume 206
Proceedings of the Environmental Science and Technology International Conference (ESTIC 2021)

Comparison of Spectral Signatures in Hyperspectral and Multispectral Data

Odontuya Gendaram[1,*], Amarsaikhan Damdinsuren[2]

[1]*Mongolian University of Pharmaceutical Sciences, Ulaanbaatar, Mongolia*
[2]*Institute of Geography and Geoecology, Mongolian Academy of Sciences, Ulaanbaatar, Mongolia*
[*]*Corresponding author. Email: odontuyag675@gmail.com*

ABSTRACT
Since the launch of the first Earth observation satellites, multispectral remote sensing (RS) datasets have been efficiently used for different thematic applications. The basis of the thematic studies is the analysis of reflecting, absorbing and emitting properties of different land surface features at different wavelengths of electro-magnetic spectrum. In other words, one should differentiate the features by their spectral signatures as observed in original data. Recently, hyperspectral datasets have been widely used for a variety of different applications. They have a number of advantages compared to multispectral data for the identification and discrimination of the features. For example, hyperspectral images have a significant adavantage over the trandtional optical images in land cover mapping, color enhancement of the Earth's objects and many others. The aim of this research is to compare the spectral signature characteristics of different land surface features in hyperspectral and multispectral images. For this purpose, Hyperion and Sentinel-2 images of Mongolia have been used. The results indicated that compared to the traditional multichannel data, the hyperspectral image could accurately differentiate the spectral characteristics of similar land cover types.

Keywords: *Hyperspectral, multispectral, spectral signatures, land surface features*

1. INTRODUCTION

Generally, Generally, the hyperspectral RS deals with a large number of bands and the datasets are formed as collections of hundreds of images of the same scene with each image corresponding to a narrow interval of the electro-magnetic wavelength [1]. With a huge number of fine spectral bandwidths, the identification of specific conditions and characteristics is greater. Developers of hyperspectral sensors provide flexible and customizable options for the number and resolution of spectral bands in the visible, near-infrared and middle-infrared portions of electro-magnetic spectrum [2].

Traditionally, multispectral RS deals with the acquisition of optical images in several broad wavelength bands. Different Earth's surface features reflect, absorb and emit differently at different wavelengths and it is possible to discriminate among the features by their spectral signatures as observed in the acquired images [3]. However, hyperspectral images have more advantages than multispectral data for the identification and discrimination of target features or object classes. They provide detailed information about any object because of narrow-band information acquisition [4].

The amount of energy from a surface can be measured as a function of wavelength which is commonly referred to as spectral signature. In other words, it is a combination of reflected, absorbed and transmitted or emitted radiation by objects at different wavelengths, which can uniquely identify an object. When the amount of reflected radiation coming from the land surface is plotted over a range of wavelengths, the connected points produce a curve which is known as spectral signature of the observed features. Differences among spectral signatures of Earth's features are used for differentiating remotely sensed scenes, since the spectral signatures of similar features have similar shapes [5].

The aim of this study is to compare the spectral signature characteristics of different land surface features in hyperspectral and multispectral images.

For this purpose, 242 band Hyperion and 13 band Sentinel-2 images of central Mongolia have been used. For the analysis, ENVI 5.2 system has been used. The results indicated that compared to the traditional multichannel data, the hyperspectral image could precisely describe the spectral characteristics of land cover types and differentiate very similar classes.

2. TEST SITE AND DATA SOURCES

As a test site, different land cover features of Ulaanbaatar, the capital city of Mongolia have been selected. Although, Ulaanbaatar is extended from the west to the east about 46km and from the north to the south about 34km, the study area chosen for the present study covers more central and southern parts of the capital city. It extends from the west to the east about 5km and from the north to the south about 6.2km. Figure 1 shows a Hyperion image of the test site, and available land cover types. In the present study, we used Hyperion image of 2002 and Sentinel-2 data of 2017. Hyperion is a high resolution hyperspectral imaging instrument that can image the land surface features in 242 spectral bands, covering the range from 0.4 µm to 2.5 µm with a ground resolution of 30 m [6].

Figure 1. Hyperion image of the test area (1-flora, 2-salix, 3-coniferous forest, 4-deciduos forest, 5-soil, 6-urban area, 7-ger area, 8-water)

For the analysis, the original Hyperion dataset was reduced from 242 bands to 173 after the bands with totally zero values were excluded. Sentinel-2 is an Earth observation mission from the Copernicus Program that systematically acquires multispectral imagery at high spatial resolution (10m-60m). The mission supports global land observation with high revisit capability to provide enhanced continuity of data so far provided by other commercially available satellites. It comprises a constellation of two polar-orbiting satellites placed in the same sun-synchronous orbit, phased at 180° to each other [7]. For the comparision analysis, mean, maximum and minimum values as well as standard deviations of the selected spectral signatures have been applied.

3. RESULT AND DISCUSSION

In the selected area of the city we have 2 urban (i.e. builtup area and ger area), four green (i.e. deciduous forest, coniferous forest, salix, flora), as well as soil and water classes. There was a high spectral mixture among the classes.

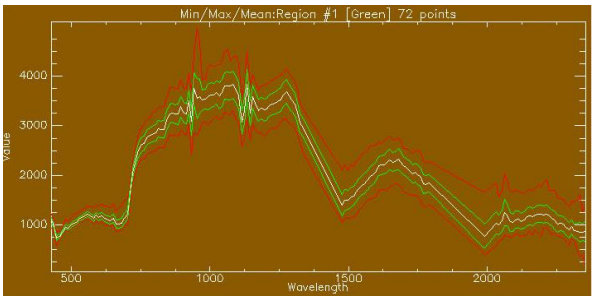

Figure 2. Spectral signature of flora

Among the selected land cover classes, flora has an interesting spectral signature (Figure 2). In the Figure 2, a white line indicates mean reflectance value, while green lines indicate standard deviations. Here, red lines show maximum and minimum reflectance values of the selected class. In case of the flora, chlorophyll strongly absorbs radiation in the red and blue wavelengths but reflects green wavelength. It appears to be the greenest, when chlorophyll content is at its maximum. In autumn days, there is less chlorophyll in vegetation, so there is less absorption and proportionately more reflection of the red wavelength, making it to appear red or yellow [8]. As seen from the Figure 2, flora absorbs some amount of energy in overall visible range. But it has very high reflection in the near infrared portion and the reflection decreases towards the middle infrared range.

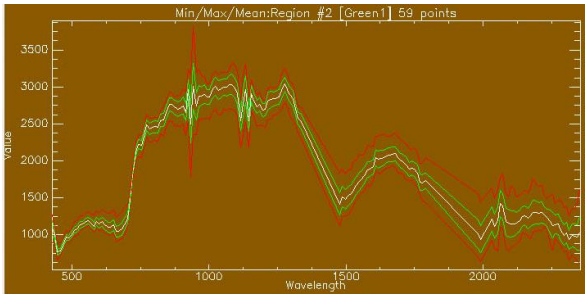

Figure 3. Spectral signature of salix

Salix has a very similar to the flora spectral reflectance (Figure 3). Both salix and flora belong to the same class as green vegetation, therefore, they have nearly the same reflecting characteristics in the visible part of the optical range. However, in the near infrared range, the salix has a lower amount of reflectance compared to the flora. This is due to the fact that in most cases, the reflectance increases to more than half because of the cell structure of the plants in the near infrared region. As a result, the latter one has the increased reflectance. In the middle infrared range 2 steep gutters are observed around 1.5 and 2.0 micrometres, because of the water absorption of the vegetation.

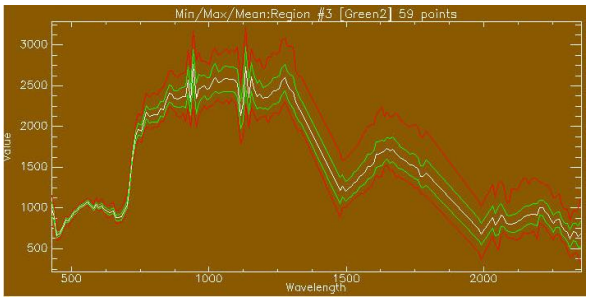

Figure 4. Spectral signature of deciduous forest

Deciduous forest has spectral reflectance similar to the flora and salix, because they belong to the same class as green vegetation (Figure 4). Although these classes have a similar shape of reflectance curve along the entire range, in the visible part, maximum values of the deciduous forest are distributed nearby the mean curve. In the near infrared portion, the curve shape is very similar to the flora shape. However, starting from 1.35 micrometres, maximum values of the deciduous forest are dispersed in more distant space from the mean curve.

As forest class, coniferous forest should have a reflectance curve similar to the deciduous forest (Figure 5). As seen from the Figure 4, both classes have almost similar reflectance in the visible spectrum. But they vary in the near and middle infrared regions, where coniferous trees have lower reflectance than deciduous trees.

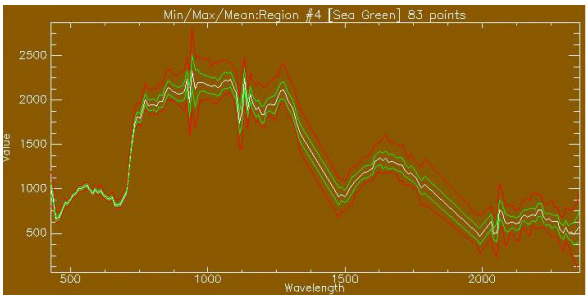

Figure 5. Spectral signature of coniferous forest

Here, the reflectance spectrum also depends on other factors such as the leaf moisture content, physical, chemical characteristics and health of the trees.

Generally, soil class has reflection properties that increase nearly monotonically with wavelength (Figure 6). As seen from the Figure 5, the soil class has highly dispersed standard deviation as well as maximum and minimum values. In most cases, especially if light soil is under consideration, it has high reflectance in all bands. This is evidently dependent on factors such as the colour, constituents and especially the moisture content.

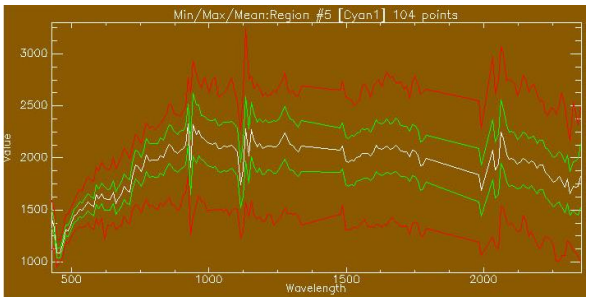

Figure 6. Spectral signature of soil

In the soil, water is durable absorber at all wavelengths, particularly those longer than the red part of the visible light. Consequently, as moisture content of the soil increases, the overall reflectance of that soil tends to decline. This means that the existence of soil moisture decreases the reflectaning capability of the soil at all visible spectrum and it continues until the soil moisture has no effect on reflectance.

In case of the urban area, knowledge of its spectral characteristics and surface objects/materials as well as other important characteristics of the additional urban factors are vital for further spectral analysis of hyperspectral datasets. As a mixture of different materials but dominated by the soil characteristics, the urban class has reflection

properties that increase virtually monotonically with wavelength (Figure 7). As seen from the Figure 6, unlike the soil class described above, it has tightly distributed standard deviation. In addition, it is seen that in the visible range the maximum and minimum values are close to the mean. However, these values are getting more dispersed starting from 0.95 micrometres along the entire near and middle infrared ranges.

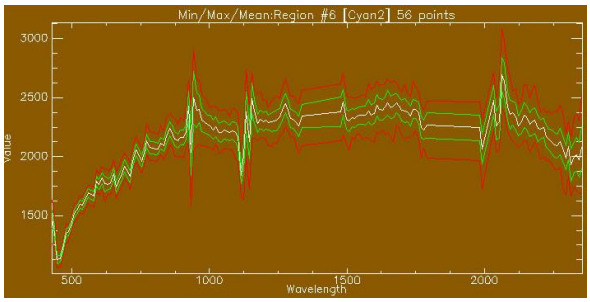

Figure 7. Spectral signature of urban area

As one of the main urban classes, specific to the Mongolian condition, ger area (Figure 8) could have reflection properties similar to the urban area. As seen from the Figure 8, these 2 classes indeed have similar spectral characteristics. However, accurate investigation of the analysis shows that in the visible range the urban class has more reflection than the ger area. Nevertheless, when it comes to the infrared portion, the latter has stronger reflection along the entire range. Moreover, it is seen that the ger area has more scattered maximum values starting from 1.5 micrometres along all ranges of infrared spectrum.

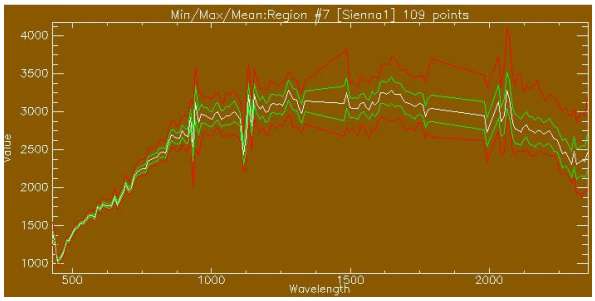

Figure 8. Spectral signature of ger area

Water has the lowest spectral reflection compared to all other classes (Figure 9) because, the longer wavelength visible and near infrared radiation is absorbed more by water. In other words, the majority of the radiant flux incident upon water is not reflected but is either absorbed or transmitted. Generally, water looks blue or blue-green due to stronger reflectance at these shorter wavelengths, and darker at red or near infrared portions. If there is deferred sediment present in the upper layer of the water body, then this will allow better reflectivity having brighter appearance of the water.

As seen from the figure, a reflectance curve of the water class is gradually decreased starting from the red range, and at the end of the middle infrared portion it absorbs almost all of the incoming radiation. Moreover, it is seen that the water body has highly dispersed standard deviation starting from the edge of red and near infrared reflectance and also very scattered maximum values along the entire infrared range.

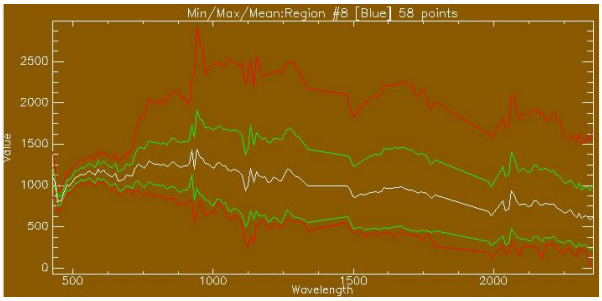

Figure 9. Spectral signature of water

Comparison of spectral signature characteristics of the available classes is shown in Figure 10. As seen from the figure, in the visible range, soil and two urban classes have the highest reflectance values, while in the infrared portion, the flora has the highest radiation. However, in the middle infrared range the soil class has very high reflectance compared to all other classes.

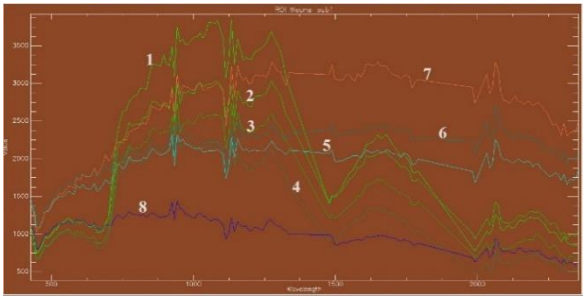

Figure 10. Spectral signatures of all classes in the Hyperion image

One of the objectives of this research was to compare the spectral signature characteristics of the selected land cover types in the Hyperion image with the same cover types in the Sentinel-2 image.

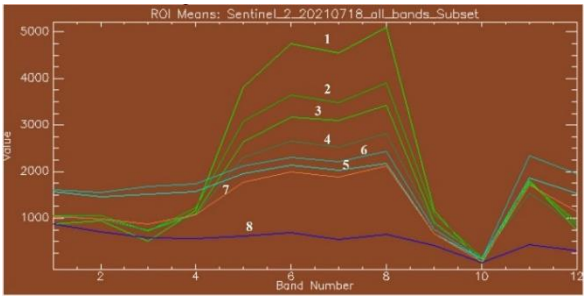

Figure 11. Spectral signatures of all classes in the Sentinel-2 image

The spectral signatures of all classes in the Sentinel-2 image are shown Figure 11. As seen from the Figure 10, unlike in the hyperspectral dataset, spectral signature curves of all classes are just connected lines. In addition, the signature characteristics not accurate.

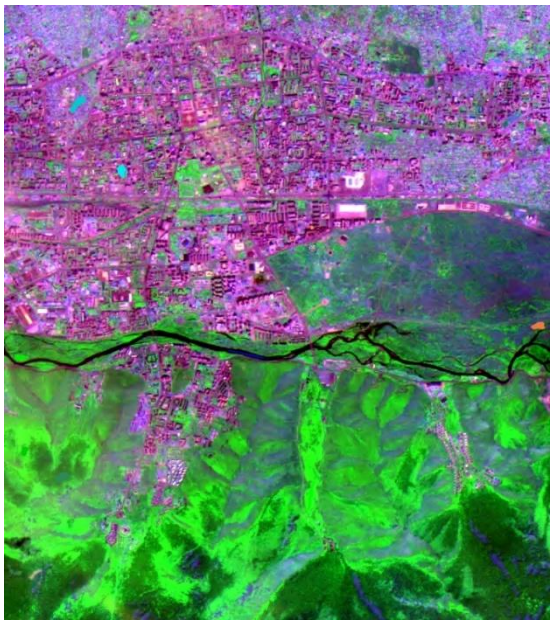

Figure 12. Sentinel-2 image of the test area

Especially, in the visible and middle infrared ranges, spectral signatures of two urban classes are very similar. Meanwhile, in the same range, the remaining six classes have similar appearances too. Nevertheless, in the near infrared range the selected classes have some separations. The Sentinel-2 image of the test area is shown Figure 12.

4. CONCLUSIONS

The aim of this research was to compare the spectral signature characteristics of different land surface features in hyperspectral and multispectral images. For this purpose, Hyperion and Sentinel-2 images related to the central part of Mongolia were used. As seen from the analysis, spectral reflectance curves of the features in the Hyperion thoroughly traced along the entire ranges of the visible and infrared spectrum, compared to the features of the Sentinel-2 that represented only averaged reflectance values. Overall the study demonstrated that compared to the traditional multichannel datasets, the hyperspectral images could accurately differentiate the spectral characteristics of similar land cover types, and successfully used for the improved land cover mapping and other thematic applications.

REFERENCES

[1] Amarsaikhan, D. and Saandar, M., 2011, Chapter 8 - "Fusion of Multisource Images for Update of Urban GIS" in "Image Fusion and Its Applications" BOOK published by InTECH Open Access Publisher, pp.127-152. DOI: https://doi.org/10.5772/16293

[2] Green, D.R., Hagon, J. and Gregory, G., 2019, Chapter 21 - Using Low-Cost UAVs for Environmental Monitoring, Mapping, and Modelling: Examples From the Coastal Zone, Coastal Management-Global Challenges and Innovations, pp. 465-501. DOI: https://doi.org/10.1016/B978-0-12-810473-6.00022-4

[3] Amarsaikhan, D., Enkhjargal, D., Bolor, G., Battsengel, V., Tsogzol, G. and Jargaldalai, E., 2015, Applications of multitemporal RS images for the evaluation of urbanization process in Mongolia, Full paper published in CD-ROM Proceedings of the ACRS, Manila, Philippines.

[4] Singh, P., Pandey, P.C., Petropoulos, G.P., 2020, Hyperspectral remote sensing in precision agriculture: present status, challenges, and future trends DOI: https://doi.org/10.1016/B978-0-08-102894-0.00009-7

[5] NASA, 2013, Landsat 7 Science Data User's Handbook. Available at http://landsathandbook.gsfc.nasa.gov.

[6] EO-1, 2017, EO1 Trajectory Details, National Space Science Data Center of NASA, Available at: https://nssdc.gsfc.nasa.gov/.

[7] Sentinel-2, 2020, Copernicus: Sentinel-2 - Satellite Missions, Available at: https://sentinel.esa.int/web/sentinel/missions/sentinel-2/satellite-description/orbit.

[8] Ruby, J.G. and Fischer, R.L., 2002, Spectral signatures database for remote sensing applications", Proc. SPIE 4816, Imaging Spectrometry VIII, DOI: https://doi.org/10.1117/12.453793